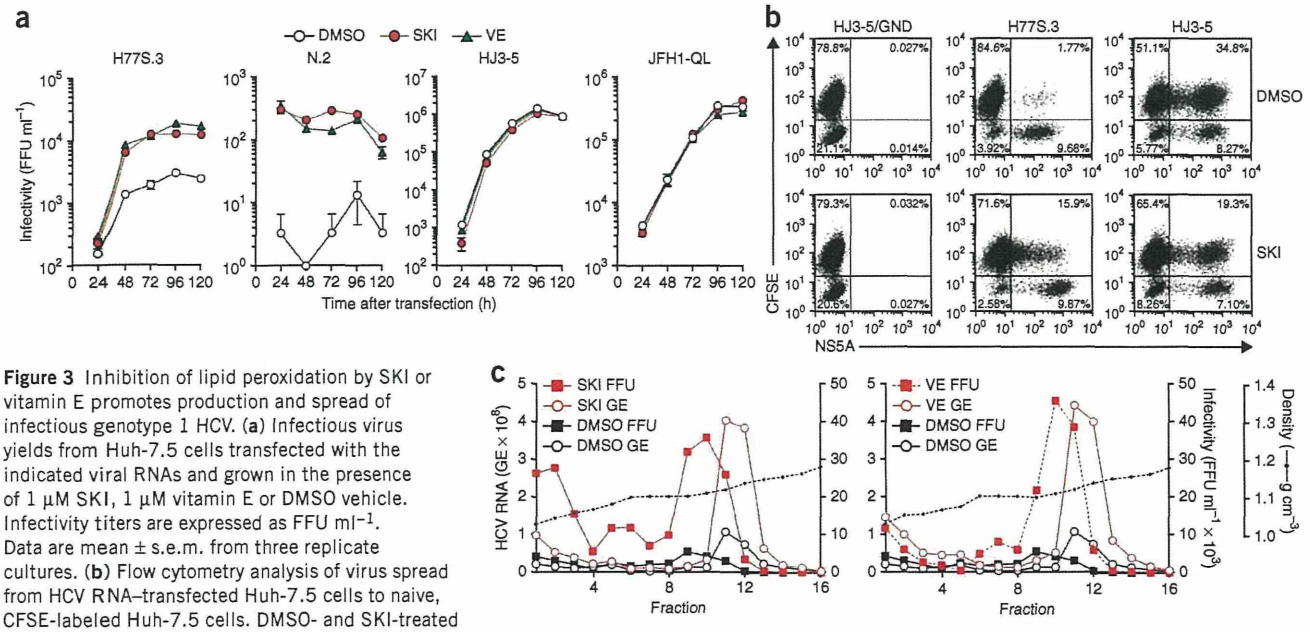

Figure 3 Inhibition of lipid peroxidation by SKI or vitamin E promotes production and spread of infectious genotype 1 HCV. (**a**) Infectious virus yields from Huh-7.5 cells transfected with the indicated viral RNAs and grown in the presence of 1 μM SKI, 1 μM vitamin E or DMSO vehicle. Infectivity titers are expressed as FFU ml^{-1}. Data are mean ± s.e.m. from three replicate cultures. (**b**) Flow cytometry analysis of virus spread from HCV RNA–transfected Huh-7.5 cells to naive, CFSE-labeled Huh-7.5 cells. DMSO- and SKI-treated cultures are shown for each transfected RNA. Percentages represent the percentage of all cells in each quadrant. $CFSE^+NS5A^+$ cells (upper right quadrant) are indicative of virus spread. (**c**) Buoyant density of H77S.3 virus particles released from H77S.3 RNA–transfected Huh-7.5 cells grown in 1 μM SKI (left) or 1 μM vitamin E (right) versus DMSO control. Fractions from isopycnic iodixanol gradients were assayed for infectious virus (FFU) or HCV RNA (GE, genome equivalents). Data are representative of two independent experiments.

that both act via a common antioxidant mechanism. Antioxidants that are not soluble in lipids, such as ebselen and *N*-acetylcysteine, as well as the NADPH oxidase inhibitor diphenyleneiodonium, had very little effect on H77S.3/GLuc replication (**Supplementary Fig. 5g**), whereas cumene hydroperoxide (CHP), a lipophilic oxidant, suppressed H77S.3/GLuc replication in a vitamin E–reversible fashion (**Fig. 2h**). FBS contains substantial quantities of lipophilic antioxidants[8]. H77S.3/GLuc replication was 20-fold lower in FBS-free cultures but was enhanced 100-fold with either SKI or vitamin E (**Fig. 2i**). HJ3-5/GLuc replication was relatively unimpaired in FBS-free medium. Collectively, these data provide evidence that endogenous lipid peroxidation restricts H77S.3/GLuc and N.2/GLuc replication, whereas the JFH1 replicase is resistant to both endogenous and chemically induced lipid peroxidation.

Endogenous lipid peroxidation restricts infectious HCV yield

Both SKI and vitamin E induced a tenfold increase in the yield of infectious virus released by H77S.3 RNA–transfected cells, reaching ~20,000 focus-forming units per milliliter (FFU ml^{-1}) (**Fig. 3a** and **Supplementary Fig. 6a**). Infectious N.2 virus yields were increased up to 100-fold (**Fig. 3a**). SKI also enhanced virus spread when we cultured H77S.3 RNA–transfected cells with nontransfected carboxyfluorescein succinimidyl ester (CFSE)-labeled cells (**Fig. 3b**). In contrast, neither SKI nor vitamin E enhanced infectious yields of JFH1-QL or HJ3-5 viruses (**Fig. 3a**), whereas SKI reduced the spread of HJ3-5 virus by >40% (**Fig. 3b**).

HCV particles produced in cell culture have heterogeneous buoyant densities[30]. However, most H77S.3 particles produced in the absence of SKI or vitamin E banded between 1.12 and 1.14 g cm^{-3} in isopycnic gradients, with peak infectivity banding between 1.10 and 1.11 g cm^{-3} (**Fig. 3c**). Neither SKI nor vitamin E altered the distribution of RNA-containing or infectious particles in gradients, but they substantially increased the abundance of both (**Fig. 3c**). SKI and vitamin E also caused modest increases in the maximum specific infectivity of virus particles (**Supplementary Fig. 6b**). Thus, SKI and vitamin E act primarily on replication of H77S.3 RNA, leading to enhanced production of infectious virus.

Lipid peroxidation restricts HCV in primary hepatocytes

To assess replication of wild-type HCV genomes possessing no cell culture–adaptive mutations, we inserted a GLuc sequence into infectious molecular clones of H77c and N[31,32]. Both H77c/GLuc and N/GLuc RNAs produced more GLuc in electroporated cells than RNA with a lethal mutation in NS5B, H77c/GLuc-AAG (**Fig. 4a**). GLuc secretion produced by either RNA was eliminated by direct-acting antivirals (DAA) targeting NS5B, confirming it represents genuine viral replication. Treatment with either SKI or vitamin E markedly increased GLuc production, whereas linoleic acid decreased GLuc secretion to background (**Fig. 4a**). Moreover, the inhibitory effect of linoleic acid was reversed by cotreatment with SKI or vitamin E. In contrast, GLuc production by wild-type JFH1/GLuc was not affected by SKI, vitamin E or linoleic acid (**Fig. 4b**). Thus, endogenous lipid peroxidation is a critical restriction factor for H77c and N viruses but not for wild-type JFH1.

To assess the effects of SKI and vitamin E on HCV replication in cells that are closely related to those naturally infected by the virus, we studied primary human fetal hepatoblasts (HFHs). SKI and vitamin E significantly increased replication of the H77S.3/GLuc reporter virus in HFHs ($P < 0.0001$ by two-way analysis of variance (ANOVA) with Holm-Sidak correction for multiple comparisons), sustaining GLuc expression for 7 d after low-multiplicity infection (**Fig. 4c,d**). In contrast, linoleic acid suppressed H77S.3 infection in HFHs in a vitamin E–reversible manner (**Fig. 4d**). Whereas H77S.3/GLuc replicated efficiently in the presence of vitamin E or SKI, HJ3-5/GLuc replication was inhibited by SKI ($P < 0.001$ by two-way ANOVA with Holm-Sidak correction for multiple comparisons) and to a lesser extent by vitamin E

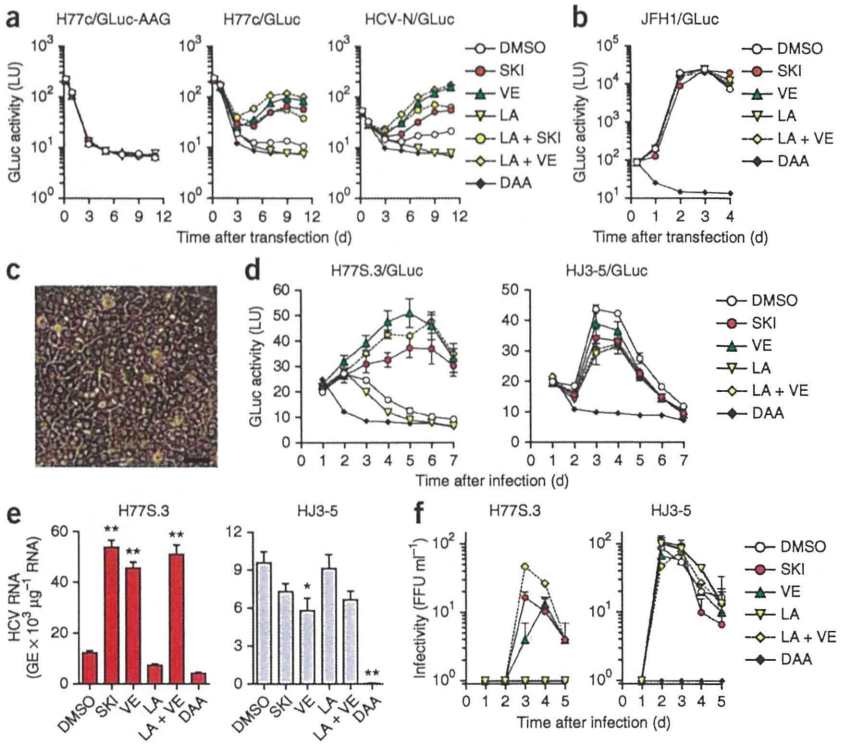

Figure 4 Lipid peroxidation regulates wild-type HCV replication and represses cell culture–adapted virus in primary human liver cultures. (**a**) Effects of SKI or vitamin E (each 1 μM), linoleic acid (20 μM), linoleic acid + SKI, linoleic acid + vitamin E or a DAA (MK-0608, 10 μM) on replication of wild-type H77c/GLuc or HCV-N/GLuc RNAs or a replication-defective control (H77c/GLuc-AAG) in Huh-7.5 cells. (**b**) Effects of SKI, vitamin E and linoleic acid (as in **a**) on replication of wild-type JFH1/GLuc RNA. DAA, PSI-6130 (10 μM). (**c**) Phase contrast microscopy of fetal hepatoblasts at 3 d. Scale bar, 50 μm. (**d**) HFHs infected with H77S.3/GLuc or HJ3-5/GLuc viruses (multiplicity of infection (MOI) = 0.001) in HFH medium containing SKI or vitamin E (each 1 μM), linoleic acid (50 μM), linoleic acid + vitamin E or a DAA (MK-0608 or PSI-6130, 10 μM) and assayed for GLuc. Results represent mean ± s.e.m. from three replicate cultures with cells from two donors. $P < 0.0001$ for SKI, VE and LA + VE compared to DMSO at 5–7 d, two-way ANOVA with Holm-Sidak correction for multiple comparisons. (**e**) HFHs infected with H77S.3 or HJ3-5 (MOI = 0.01) and treated as in **d**. Cell-associated viral RNA was quantified by quantitative RT-PCR (qRT-PCR) at 5 d (*$P < 0.05$, **$P < 0.001$ by two-way ANOVA. GE, genome equivalent. (**f**) Infectious virus released from H77S.3 or HJ3-5 virus–inoculated HFHs (MOI = 0.01). Virus was quantified by FFU assay. Results represent mean ± s.e.m. from three replicate cultures.

($P < 0.05$) (**Fig. 4d**). We observed similar results in cells infected with H77S.3 or HJ3-5 viruses lacking a GLuc insertion (**Fig. 4e**). We detected production of infectious H77S.3 virus in HFH cultures only in the presence of vitamin E or SKI and found that infectious HJ3-5 yields were not enhanced by either treatment (**Fig. 4f**). Whereas the disruption of innate immune responses is known to promote HCV replication in HFHs[33], neither SKI nor vitamin E reduced Sendai virus activation of the interferon-β promoter (**Supplementary Fig. 7**). Thus, SKI and vitamin E do not promote H77S.3 replication in HFHs by blocking activation of the interferon response to virus infection.

Lipid peroxidation reduces the EC_{50} of direct antivirals

Both SKI and vitamin E treatment increased the area occupied by the membranous web in H77S.3-infected cells (**Fig. 5a,b**) without altering the morphology of double-membrane vesicles, which are the likely site of genome replication[14]. Increased lipid peroxidation reduced the area occupied by the membranous web, whereas the HJ3-5 membranous web was insensitive to changes in lipid peroxidation.

Reverse molecular genetic studies involving exchanges between the H77S.3 and JFH1 genomes suggested that the peroxidation resistance phenotype of JFH1 involves multiple nonstructural proteins within the replicase (**Supplementary Results** and **Supplementary Fig. 8**). Consistent with this, we observed an unexpected increase in the 50% effective concentration (EC_{50}) of DAAs targeting the NS3-4A protease (a noncovalent complex of NS3 and its cofactor, NS4A) and NS5B polymerase after suppressing endogenous lipid peroxidation in H77S.3/GLuc-infected cells (**Fig. 5d,e** and **Supplementary Fig. 9a–c**). Both SKI and vitamin E masked the antiviral effects of PSI-6130, a potent NS5B inhibitor (**Fig. 5c**), in part owing to an increase in its EC_{50} from 3.49 μM (95% confidence interval (CI) 2.48–4.89) to 6.22 μM (4.43–8.72) and 8.46 μM (7.60–9.44), respectively (**Fig. 5d**). SKI and vitamin E also increased the EC_{50} of MK-7009, an inhibitor of the NS3-4A protease, from 0.488 nM (95% CI 0.411–0.578) to 1.45 nM (1.23–1.72) and 1.90 nM (1.64–2.22), respectively (**Fig. 5e**). The EC_{50} values of other inhibitors targeting NS3-4A (boceprevir) and NS5B (HCV-796 and MK-0608) were similarly increased against H77S.3/GLuc by SKI and vitamin E, but neither SKI nor vitamin E significantly altered the EC_{50} of SCY-635, cyclosporine A, compound 23 or a locked nucleic acid–modified oligonucleotide complementary to miR-122 (anti–miR-122), inhibitors targeting essential HCV host factors, or interferon-α (**Fig. 5f,g** and **Supplementary Fig. 9d–g**). In contrast, SKI and vitamin E caused no change in the EC_{50} of any antiviral against HJ3-5/GLuc (**Fig. 5d,g** and **Supplementary Fig. 9a–f**), indicating that vitamin E and SKI do not impair cellular uptake or metabolism of DAAs. These changes in the EC_{50} against H77S.3/GLuc thus probably reflect altered affinity of the DAAs for NS3-4A and NS5B, suggesting that peroxidation modulates the conformation of these replicase proteins.

Resistance to lipid peroxidation maps to NS4A and NS5B

TNcc is a recently described genotype 1a virus with eight cell culture–adaptive mutations that replicates almost as well as JFH1 in Huh-7.5 cells[34]. Notably, we found it completely resistant to lipid peroxidation (**Fig. 6a** and **Supplementary Fig. 10a**). We introduced all eight TNcc mutations into H77S.3 to determine whether they would confer peroxidation resistance. This RNA (H77S.3/$GLuc_{8mt}$) failed to replicate, but removal of a key H77S.3 adaptive mutation (S2204I in NS5A)[12] restored low-level replication. The resulting virus, H77S.3/$GLuc_{IS/8mt}$, was resistant to lipid peroxidation (**Fig. 6a** and **Supplementary Fig. 10b**). Continued passage of cells infected with H77S.$3_{IS/8mt}$ resulted in the emergence of viruses carrying additional mutations in NS4B (G1909S), NS5A (D2416G) and NS5B (G2963D) that together enhanced replication by 850-fold (**Supplementary Results** and **Supplementary Fig. 11**). The NS4B G1909S mutation

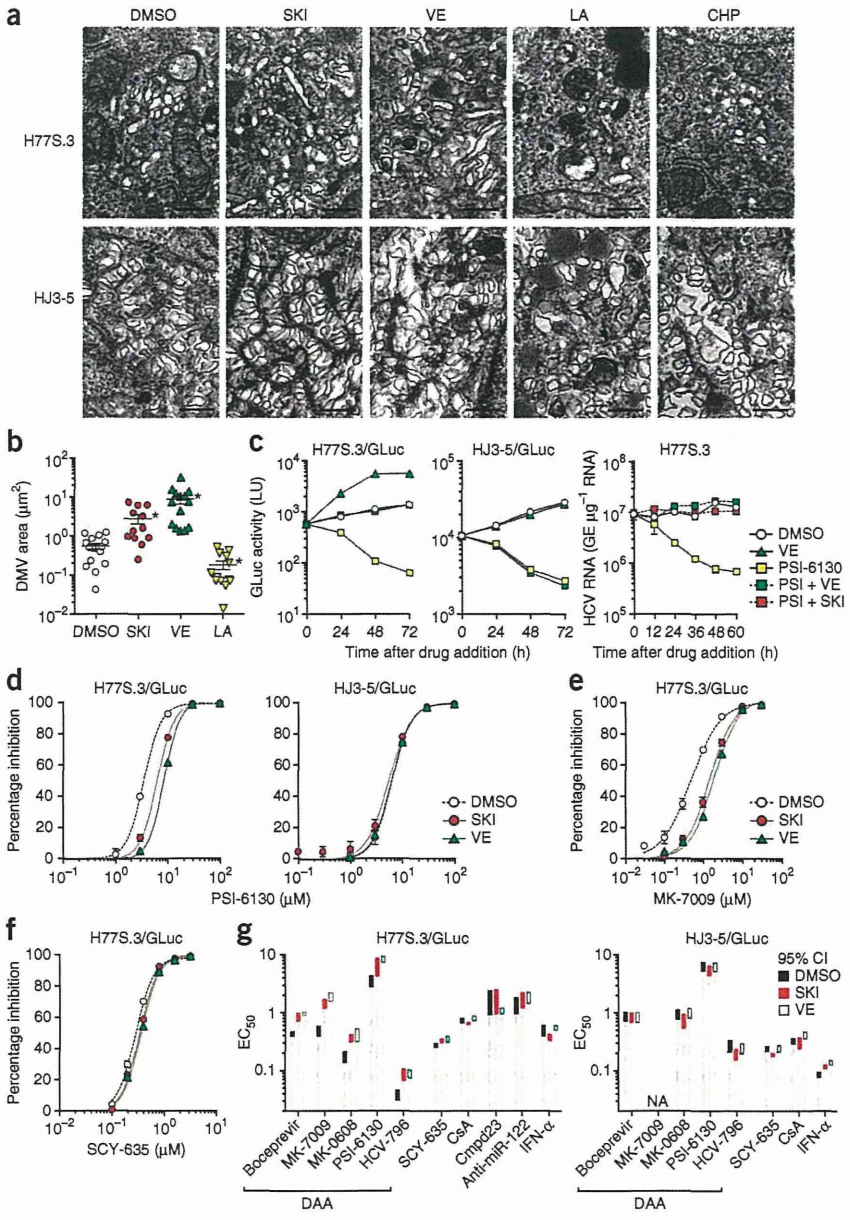

Figure 5 Lipid peroxidation reduces HCV-induced membranous web abundance and alters the EC_{50} of DAAs. (**a**) Transmission electron microscopic images of the membranous web in Huh-7.5 cells electroporated with H77S.3 or HJ3-5 RNA and treated with DMSO, SKI (1 μM), vitamin E (1 μM), linoleic acid (50 μM) or CHP (10 μM). Images shown are representative of 10 different microscopic fields. Scale bars, 500 nm. (**b**) Quantitation of area occupied by double-membrane vesicles (DMV) within individual cells infected with H77S.3 virus and treated with SKI, vitamin E or linoleic acid as in **a**. $^*P \leq 0.002$ versus DMSO by two-sided Mann-Whitney *U* test. (**c**) The effect of SKI and vitamin E on the antiviral effect of PSI-6130 against H77S.3/GLuc replication. Left and middle, GLuc produced from Huh-7.5 cells transfected with H77S.3/GLuc or HJ3-5/GLuc RNA 7 d prior to treatment with DMSO, 10 μM PSI-6130, 1 μM vitamin E or both PSI-6130 and either SKI or vitamin E. Right, Cell-associated HCV RNA in similarly treated cells transfected with H77S.3 RNA. Results represent mean ± s.e.m. from two (left, middle) or three (right) replicate cultures. (**d**) Inhibition of H77S.3 (left) and HJ3-5 (right) replication by the NS5B inhibitor PSI-6130 in the presence of SKI or vitamin E (each 1 μM) or DMSO vehicle, assessed by quantifying GLuc secreted 48–72 h after drug addition. Results represent mean ± s.e.m. of two replicate cultures. (**e**,**f**) Inhibition of H77S.3 replication by MK-7009, an NS3-4A inhibitor, (**e**) and SCY-635, a host-targeting cyclophilin inhibitor (**f**). Results represent mean ± s.e.m. of triplicate cultures. (**g**) EC_{50} values of direct-acting versus indirect-acting antivirals against H77S.3 (left) and HJ3-5 (right) viruses in the presence of SKI or vitamin E (each 1 μM). Assays were carried out as in **d**–**f**. Colored bars represent limits of the 95% CI of EC_{50} values calculated from Hill plots. NA, not measureable owing to poor antiviral activity; IFN-α, interferon-α; CsA, cyclosporine A; Cmpd23, compound 23. Additional details are shown in **Supplementary Figure 9**.

compensated for the negative effects on replication of TNcc mutations placed into the H77S.3 background (**Fig. 6b**). When we introduced all three additional mutations (G1909S, D2416G and G2963D) into H77S.3/$GLuc_{IS/8mt}$, the resulting virus (designated H77D) produced infectious virus yields comparable to those of HJ3-5 or JFH1-QL, which were not increased by vitamin E supplementation (**Fig. 6b**). Notably, the EC_{50} of DAAs against H77D virus was not altered by SKI or vitamin E (**Fig. 6d** and **Supplementary Fig. 9h**).

Introducing the G1909S mutation into H77S.3/$GLuc_{IS}$ (H77S.3/$GLuc_{IS/GS}$) did not confer peroxidation resistance (**Fig. 6a**). However, its compensatory effect on the TNcc-derived mutations allowed us to identify the A1672S mutation (in NS4A) from TNcc as essential for peroxidation resistance and to show that TNcc-derived mutations in NS3 and NS4B were not required for this phenotype (**Fig. 6a**). TNcc mutations in NS5B (D2979G, Y2981F and F2994S) were essential for replication of peroxidation-resistant virus, but neither these nor A1672S (in NS4A) alone conferred peroxidation resistance (**Supplementary Fig. 10c**). Thus, mutations in both NS4A and NS5B are required for genotype 1a peroxidation resistance. These mutations are within or in close proximity to the transmembrane domains of these proteins (**Fig. 6c**), consistent with direct involvement of these residues in resistance to lipid peroxidation.

Regulation by lipid peroxidation is unique to HCV

In addition to replication of genotypes 1a (H77S.3) and 1b (HCV-N.2) (**Figs. 2c** and **3a**), replication of HCV genotypes 2a (JFH-2), 3a (S52) and 4a (ED43) was enhanced by treatment with SKI or vitamin E and inhibited by CHP-induced lipid peroxidation (**Fig. 6e**). JFH1 is thus unique among wild-type HCV strains in its resistance to lipid peroxidation.

As with HCV, the genomes of other positive-strand RNA viruses are synthesized by replicase complexes that assemble in association with cytoplasmic membranes and are thus at risk for damage due to lipid peroxidation. Yet, like replication of JFH1, the replication of other

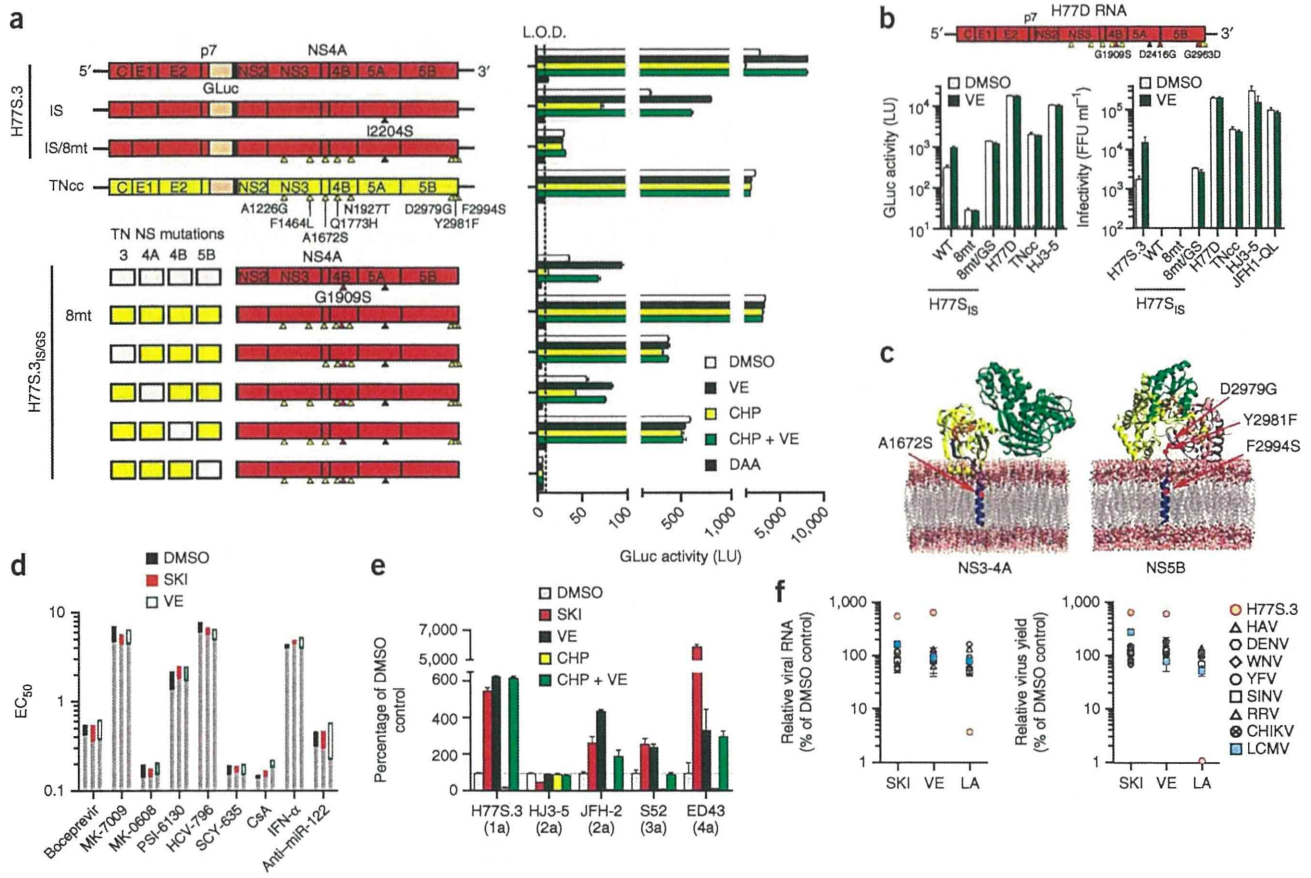

Figure 6 Resistance to lipid peroxidation is tightly linked to robust replication in cell culture. (**a**) Top, cell culture–adaptive mutations in TNcc[34] (yellow arrowheads) that confer resistance to lipid peroxidation when introduced into H77S.3/GLuc$_{IS}$ (H77S.3/GLuc, in which the adaptive mutation S2204I has been removed (black arrowheads); details are shown in **Supplementary Fig. 10b**). GLuc produced from Huh-7.5 cells transfected with indicated RNAs and treated with DMSO, 1 μM SKI, 1 μM vitamin E, 10 μM CHP, CHP plus vitamin E or 30 μM sofosbuvir (DAA). GLuc secreted between 48–72 h is shown. Bottom, role played by TNcc mutations in NS3 (helicase) and NS4B in resistance to lipid peroxidation. Combinations of TNcc substitutions were introduced into H77S.3/GLuc$_{IS/GS}$ (NS proteins shown only) that contains the compensatory mutation G1909S (GS) in NS4B (red arrowhead, **Supplementary Fig. 11**). Data represent mean GLuc activity ± s.e.m. from two independent experiments. (**b**) Top, H77D genome containing the I2204S substitution (black arrowhead), eight TNcc-derived mutations (yellow arrowheads) and three additional compensatory mutations (red arrowheads) in the H77S.3 background. Bottom, GLuc (left) and infectious virus (right) released from Huh-7.5 cells transfected with the indicated RNAs encoding GLuc (left) or lacking GLuc (right) and treated with DMSO or 1 μM vitamin E. Data represent means ± s.d. from triplicate cultures harvested between 48–72 h in a representative experiment. WT, wild-type. (**c**) Structural models of NS4A (left) and NS5B (right) membrane interactions showing key residues that determine sensitivity to lipid peroxidation. (**d**) EC_{50} of direct-acting versus indirect-acting antivirals against H77D in the presence of SKI or vitamin E (each 1 μM). Assays were carried out as in **Figure 5g**. (**e**) Huh-7.5 cells transfected with H77S.3/GLuc or HJ3-5/GLuc RNA, genome-length JFH-2 RNA or subgenomic RNAs (S52 and ED43) encoding firefly luciferase (FLuc) and treated with DMSO, 1 μM SKI or vitamin E, 10 μM CHP or CHP plus vitamin E. Data represent percentage GLuc (H77S.3 and HJ3-5), RNA copies (JFH-2) or FLuc activities (S52 and ED43) at 72 h relative to DMSO controls. Data represent mean ± s.e.m. from three independent experiments. (**f**) The impact of SKI or vitamin E (each 1 μM) or linoleic acid (50 μM) on the abundance of viral RNA (left) or yields of infectious virus (right), as determined for a panel of RNA viruses following infection of Huh-7.5 cells. Data are mean ± s.e.m. from three replicate cultures. Additional details are shown in **Supplementary Figure 12**. HAV, hepatitis A virus; DENV, dengue virus; WNV, West Nile virus; YFV, yellow fever virus; SINV, Sindbis virus; RRV, Ross River virus; CHIKV, Chikungunya virus; LCMV, lymphocytic choriomeningitis virus.

pathogenic positive-strand RNA viruses, including flaviviruses, picornaviruses and alphaviruses, is neither enhanced by SKI or vitamin E nor suppressed by linoleic acid (**Fig. 6f** and **Supplementary Fig. 12a–c**). This is also true for clone 13 lymphocytic choriomeningitis virus, an ambisense RNA virus that establishes persistent infections (**Fig. 6f** and **Supplementary Fig. 12d**). Thus, most viral RNA replicases have evolved in ways that prevent or mitigate the potentially negative effects of lipid peroxidation. HCV is a clear exception, suggesting that its sensitivity to lipid peroxidation may provide a distinct survival advantage.

DISCUSSION

Lipid peroxides are formed on polyunsaturated fatty acid chains within membranes by reactive intermediates produced during oxidative stress. They alter membrane fluidity and permeability and potentially contribute to a variety of disease states[35]. The degradation products of these lipid peroxides include reactive aldehydes, such as acrolein, 4-hydroxy-2-nonenal and MDA, that add to this damage by forming adducts with membrane proteins, thereby modulating their biological activities[35,36]. To our knowledge, the opposing effects of SPHK1 and SPHK2 on lipid peroxidation that we observed

have not been noted previously; they remain unexplained. SPHK1 is predominantly cytosolic and translocates to the plasma membrane upon activation[37], whereas SPHK2 is more likely to be associated with intracellular membranes[28]. Sphingosine-1-phosphate produced by SPHK functions as a messenger in several signaling pathways and is a cofactor for enzymes involved in signal transduction and transcriptional regulation[38,39]. However, it has no effect on HCV replication in cell cultures and only minimally increases MDA abundance (**Supplementary Fig. 1c,d**).

During HCV infection, oxidative stress is caused by both host inflammatory responses and direct interactions of viral proteins with mitochondria[7,40]. Our results show that the wild-type H77c and N replicases are highly sensitive to both endogenous and PUFA-induced lipid peroxidation. Con1 and OR6, two other genotype 1 HCVs, are also inhibited by PUFA-induced peroxidation[8,41]. Given that we found that lipid peroxidation also inhibits multiple other HCV genotypes, we conclude that this sensitivity to peroxidation is a common feature of HCV.

In genotype 1a H77S.3 virus, we found that resistance to lipid peroxidation maps to residues within or near the transmembrane domains of NS4A and NS5B, key components of the replicase complex. Reactive aldehydes derived from degraded lipid peroxides could form adducts with residues within these transmembrane domains, impairing their capacity for essential interactions and thereby reducing replicase activity. The A1672S mutation promotes oligodimerization of the NS4A transmembrane domain, an interaction necessary for efficient replicase function[42]. Thus, A1672S might confer resistance to peroxidation by restoring NS4A dimerization impaired by adduct formation. Adduct formation could similarly affect the NS5B transmembrane domain. Although hypothetical, such effects could explain the changes we observed in the EC_{50} of DAAs targeting NS3-4A and NS5B. Alternatively, proper membrane localization and assembly of nonstructural proteins within the replicase may require lipids esterified with nonoxidized fatty acid chains. Indeed, we found that monounsaturated fatty acid supplements such as oleic acid stimulate H77S.3/GLuc and N.2/GLuc replication but not that of JFH1 (**Supplementary Fig. 5h**). A third possibility is that lipid peroxidation could induce changes in membrane fluidity that alter replicase conformation[35].

We propose that HCV exploits lipid peroxidation as a means of autoregulating its replication and that lipid peroxides act as a brake, downregulating the efficiency of genome amplification when reaching a threshold abundance (**Supplementary Fig. 13**). Such a model suggests that HCV possesses a conserved peroxidation 'sensor', mapping in part to the transmembrane domains of NS4A and NS5B, that governs replication efficiency, thereby limiting tissue damage, reducing viral exposure to the immune system and facilitating viral persistence. Although hepatotoxicity associated with diets deficient in lipophilic antioxidants presents a technical barrier to testing this hypothesis in murine models of HCV[43], our results show that in primary human hepatocytes, HCV replication is regulated by lipid peroxidation. Related RNA viruses that are capable of establishing persistent infection appear to autorestrict replication via alternative mechanisms. For example, bovine viral diarrhea virus, a pestivirus that establishes lifelong persistence, downregulates replicase formation by limiting cleavage of its NS2-3 protein, thereby arresting RNA synthesis and enabling a noncytolytic phenotype[44]. Thus, reducing the efficiency of the replicase may be a common theme for RNA viruses that establish persistent infection.

Like most other positive-strand RNA viruses, the genotype 2a JFH1 virus is highly resistant to lipid peroxidation. This suggests that JFH1 may be a loss-of-function mutant that no longer senses lipid peroxides and autorestricts its replicase activity. Whether the original JFH1 patient isolate similarly lacked the ability to be regulated by lipid peroxidation is uncertain, as is the possibility that lack of peroxidation sensitivity contributed in some way to the fulminant hepatitis experienced by this patient[9]. Only one of the four amino acid substitutions conferring peroxidation resistance in H77S.3 (NS5B F2981) exists in JFH1, and the molecular basis of its peroxidation resistance remains to be determined. Nonetheless, our results provide a basis for understanding the robust capacity of the JFH1 virus to replicate in cell culture. Our findings also highlight the uniqueness of HCV regulation by lipid peroxidation among other pathogenic RNA viruses and its potential importance to the pathogenesis of chronic hepatitis C.

METHODS

Methods and any associated references are available in the online version of the paper.

Note: Any Supplementary Information and Source Data files are available in the online version of the paper.

ACKNOWLEDGMENTS

We thank L.F. Ping and W. Lovell for expert technical assistance, R. Purcell (US National Institute of Allergy and Infectious Diseases) and J. Bukh (Copenhagen University Hospital, Denmark) for pCV-H77C and pTNcc plasmids, C.M. Rice and M. Saeed (The Rockefeller University) for Huh-7.5 cells and S52/SG-Feo and ED43/SG-Feo plasmids, T. Wakita (National Institute of Infectious Diseases, Japan) for pJFH1 and pJFH-2 plasmids, M.J. Otto (Pharmasset) for PSI-6130, A. Sluder (SCYNEXIS) for SCY-635, R. De Francesco (Istituto Nazionale di Genetica Molecolare, Italy) for compound 23, A.Y. Howe (Merck Research Laboratory) for boceprevir, HCV-796, MK-0608 and MK-7009 and Z. Feng (University of North Carolina) for hepatitis A virus stocks. We also thank S.A. Weinman for critical reading of the manuscript and D.L. Tyrrell, M. Joyce, R.A. Coleman and T. Masaki for helpful discussions. This work was supported by US National Institutes of Health grants RO1-AI095690, RO1-CA164029 and U19-AI109965 (S.M.L.), R21-CA182322 (L.R.), R01-AI075090 (M.Y.), RO1-AI073335 (C.C.K.), RO1-DE018304 (D.P.D.), F32-AI094941 (D.G.W.) and U54-GM069338 (S.B.), a National Cancer Institute Center Core Support Grant to the Lineberger Comprehensive Cancer Center (P30-CA016086) and the University of North Carolina Cancer Research Fund. C.W. was supported by the Deutsche Forschungsgemeinschaft (WE 4388/3-1 and WE 4388/6-1). I.A. was supported by the CIPSM Cluster of Excellence.

AUTHOR CONTRIBUTIONS

D.Y. and S.M.L. conceived the study and wrote the paper; D.Y., D.R.M., E.W., V.J.M., Y.W., P.E.C., C.E.M., D.G.W. and I.M. conducted experiments; C.W. and I.A. modeled membrane interactions of proteins; S.B. and A.H.M. Jr. carried out mass spectrometry analysis of sphingolipids; J.K.W., M.T.H., D.P.D. and C.C.K. provided reagents and supervised experiments involving viruses other than HCV; M.Y., S.K., T.S., T.O., S.M.P. and L.M.R. provided research materials; and all authors discussed the results and commented on the manuscript.

COMPETING FINANCIAL INTERESTS

The authors declare competing financial interests: details are available in the online version of the paper.

1. Kalyanaraman, B. Teaching the basics of redox biology to medical and graduate students: oxidants, antioxidants and disease mechanisms. *Redox. Biol.* **1**, 244–257 (2013).
2. Nathan, C. & Cunningham-Bussel, A. Beyond oxidative stress: an immunologist's guide to reactive oxygen species. *Nat. Rev. Immunol.* **13**, 349–361 (2013).
3. Dennery, P.A. Effects of oxidative stress on embryonic development. *Birth Defects Res. C Embryo Today* **81**, 155–162 (2007).
4. Valyi-Nagy, T. & Dermody, T.S. Role of oxidative damage in the pathogenesis of viral infections of the nervous system. *Histol. Histopathol.* **20**, 957–967 (2005).
5. Thomas, D.L. Global control of hepatitis C: where challenge meets opportunity. *Nat. Med.* **19**, 850–858 (2013).
6. Choi, J. Oxidative stress, endogenous antioxidants, alcohol, and hepatitis C: pathogenic interactions and therapeutic considerations. *Free Radic. Biol. Med.* **52**, 1135–1150 (2012).

7. Okuda, M. *et al.* Mitochondrial injury, oxidative stress, and antioxidant gene expression are induced by hepatitis C virus core protein. *Gastroenterology* **122**, 366–375 (2002).
8. Huang, H., Chen, Y. & Ye, J. Inhibition of hepatitis C virus replication by peroxidation of arachidonate and restoration by vitamin E. *Proc. Natl. Acad. Sci. USA* **104**, 18666–18670 (2007).
9. Wakita, T. *et al.* Production of infectious hepatitis C virus in tissue culture from a cloned viral genome. *Nat. Med.* **11**, 791–796 (2005).
10. Lindenbach, B.D. *et al.* Complete replication of hepatitis C virus in cell culture. *Science* **309**, 623–626 (2005).
11. Zhong, J. *et al.* Robust hepatitis C virus infection *in vitro*. *Proc. Natl. Acad. Sci. USA* **102**, 9294–9299 (2005).
12. Yi, M., Villanueva, R.A., Thomas, D.L., Wakita, T. & Lemon, S.M. Production of infectious genotype 1a hepatitis C virus (Hutchinson strain) in cultured human hepatoma cells. *Proc. Natl. Acad. Sci. USA* **103**, 2310–2315 (2006).
13. Pietschmann, T. *et al.* Production of infectious genotype 1b virus particles in cell culture and impairment by replication enhancing mutations. *PLoS Pathog.* **5**, e1000475 (2009).
14. Paul, D., Hoppe, S., Saher, G., Krijnse-Locker, J. & Bartenschlager, R. Morphological and biochemical characterization of the membranous hepatitis C virus replication compartment. *J. Virol.* **87**, 10612–10627 (2013).
15. Gosert, R. *et al.* Identification of the hepatitis C virus RNA replication complex in Huh-7 cells harboring subgenomic replicons. *J. Virol.* **77**, 5487–5492 (2003).
16. Shi, S.T., Lee, K.J., Aizaki, H., Hwang, S.B. & Lai, M.M. Hepatitis C virus RNA replication occurs on a detergent-resistant membrane that cofractionates with caveolin-2. *J. Virol.* **77**, 4160–4168 (2003).
17. Hsu, N.Y. *et al.* Viral reorganization of the secretory pathway generates distinct organelles for RNA replication. *Cell* **141**, 799–811 (2010).
18. Reiss, S. *et al.* Recruitment and activation of a lipid kinase by hepatitis C virus NS5A is essential for integrity of the membranous replication compartment. *Cell Host Microbe* **9**, 32–45 (2011).
19. Saxena, V., Lai, C.K., Chao, T.C., Jeng, K.S. & Lai, M.M. Annexin A2 is involved in the formation of hepatitis C virus replication complex on the lipid raft. *J. Virol.* **86**, 4139–4150 (2012).
20. Romero-Brey, I. *et al.* Three-dimensional architecture and biogenesis of membrane structures associated with hepatitis C virus replication. *PLoS Pathog.* **8**, e1003056 (2012).
21. Miyanari, Y. *et al.* The lipid droplet is an important organelle for hepatitis C virus production. *Nat. Cell Biol.* **9**, 1089–1097 (2007).
22. Aizaki, H. *et al.* Critical role of virion-associated cholesterol and sphingolipid in hepatitis C virus infection. *J. Virol.* **82**, 5715–5724 (2008).
23. Sakamoto, H. *et al.* Host sphingolipid biosynthesis as a target for hepatitis C virus therapy. *Nat. Chem. Biol.* **1**, 333–337 (2005).
24. Umehara, T. *et al.* Serine palmitoyltransferase inhibitor suppresses HCV replication in a mouse model. *Biochem. Biophys. Res. Commun.* **346**, 67–73 (2006).
25. Hirata, Y. *et al.* Self-enhancement of hepatitis C virus replication by promotion of specific sphingolipid biosynthesis. *PLoS Pathog.* **8**, e1002860 (2012).
26. Weng, L. *et al.* Sphingomyelin activates hepatitis C virus RNA polymerase in a genotype-specific manner. *J. Virol.* **84**, 11761–11770 (2010).
27. Shimakami, T. *et al.* Protease inhibitor-resistant hepatitis C virus mutants with reduced fitness from impaired production of infectious virus. *Gastroenterology* **140**, 667–675 (2011).
28. Liu, H. *et al.* Molecular cloning and functional characterization of a novel mammalian sphingosine kinase type 2 isoform. *J. Biol. Chem.* **275**, 19513–19520 (2000).
29. Kapadia, S.B. & Chisari, F.V. Hepatitis C virus RNA replication is regulated by host geranylgeranylation and fatty acids. *Proc. Natl. Acad. Sci. USA* **102**, 2561–2566 (2005).
30. Lindenbach, B.D. *et al.* Cell culture-grown hepatitis C virus is infectious *in vivo* and can be recultured *in vitro*. *Proc. Natl. Acad. Sci. USA* **103**, 3805–3809 (2006).
31. Yanagi, M., Purcell, R.H., Emerson, S.U. & Bukh, J. Transcripts from a single full-length cDNA clone of hepatitis C virus are infectious when directly transfected into liver of a chimpanzee. *Proc. Natl. Acad. Sci. USA* **94**, 8738–8743 (1997).
32. Beard, M.R. *et al.* An infectious molecular clone of a Japanese genotype 1b hepatitis C virus. *Hepatology* **30**, 316–324 (1999).
33. Andrus, L. *et al.* Expression of paramyxovirus V proteins promotes replication and spread of hepatitis C virus in cultures of primary human fetal liver cells. *Hepatology* **54**, 1901–1912 (2011).
34. Li, Y.P. *et al.* Highly efficient full-length hepatitis C virus genotype 1 (strain TN) infectious culture system. *Proc. Natl. Acad. Sci. USA* **109**, 19757–19762 (2012).
35. Bochkov, V.N. *et al.* Generation and biological activities of oxidized phospholipids. *Antioxid. Redox Signal.* **12**, 1009–1059 (2010).
36. Pizzimenti, S. *et al.* Interaction of aldehydes derived from lipid peroxidation and membrane proteins. *Front. Physiol.* **4**, 242 (2013).
37. Pitson, S.M. *et al.* Activation of sphingosine kinase 1 by ERK1/2-mediated phosphorylation. *EMBO J.* **22**, 5491–5500 (2003).
38. Alvarez, S.E. *et al.* Sphingosine-1-phosphate is a missing cofactor for the E3 ubiquitin ligase TRAF2. *Nature* **465**, 1084–1088 (2010).
39. Hait, N.C. *et al.* Regulation of histone acetylation in the nucleus by sphingosine-1-phosphate. *Science* **325**, 1254–1257 (2009).
40. Jain, S.K. *et al.* Oxidative stress in chronic hepatitis C: not just a feature of late stage disease. *J. Hepatol.* **36**, 805–811 (2002).
41. Yano, M. *et al.* Comprehensive analysis of the effects of ordinary nutrients on hepatitis C virus RNA replication in cell culture. *Antimicrob. Agents Chemother.* **51**, 2016–2027 (2007).
42. Kohlway, A. *et al.* Hepatitis C virus RNA replication and virus particle assembly require specific dimerization of the NS4A protein transmembrane domain. *J. Virol.* **88**, 628–642 (2014).
43. Ibrahim, W. *et al.* Oxidative stress and antioxidant status in mouse liver: effects of dietary lipid, vitamin E and iron. *J. Nutr.* **127**, 1401–1406 (1997).
44. Lackner, T., Muller, A., Konig, M., Thiel, H.J. & Tautz, N. Persistence of bovine viral diarrhea virus is determined by a cellular cofactor of a viral autoprotease. *J. Virol.* **79**, 9746–9755 (2005).

ONLINE METHODS

Cells and reagents. Huh-7.5 cells were grown in Dulbecco's modified Eagle's medium (DMEM), High Glucose supplemented with 10% fetal bovine serum (FBS), 1× penicillin-streptomycin, 1× GlutaMAX and 1× MEM Non-Essential Amino Acids Solution (Gibco). BD-BioCoat collagen-I coated plates were purchased from BD Biosciences. SKI (2-(*p*-hydroxyanilino)-4-(*p*-chlorophenyl) thiazole) was obtained from Merck Millipore. Myriocin, fumonisin B1, *N*-[2-hydroxy-1-(4-morpholinylmethyl)-2-phenylethyl]-decanamide (PDMP), D-erythro-2-tetradecanoylamino-1-phenyl-1-propanol (D-MAPP), dihydrosphingosine, C-2 and C-8 ceramides, sphingosine, sphingosine 1-phosphate, lovastatin, ebselen, arachidonic acid, docosahexaenoic acid and linoleic acid were from Cayman Chemical. Vitamin E (α-, *rac*-β- and γ-tocopherols), 4-deoxypyridoxine hydrochloride (DOP), coenzyme Q10, butylated hydroxytoluene, *N*-acetyl-L-cysteine, diphenyleneiodonium chloride, oleic acid and cyclosporine A were from Sigma-Aldrich. nSMase spiroepoxide and cumene hydroperoxide were from Santa Cruz Biotechnology; D609 was from Enzo Life Sciences; and sofosbuvir (PSI-7977) was from Chemscene. Locked nucleic acid anti-miR-122 was synthesized by Exiqon. A selective PI4KIIIα inhibitor, compound 23 (ref. 45), was provided by R. De Francesco. Relative cell numbers were assessed using the WST-1 reagent (Millipore) or determination of protein content. Protein concentrations in samples were determined using the Protein Assay kit (Bio-Rad) with bovine serum albumin as a standard.

Fetal liver cells. Tissue samples were supplied by the accredited nonprofit corporation Advanced Biosciences Resources, Inc. (ABR) and obtained from fetuses between 15–20 weeks gestation during elective terminations of pregnancy. Tissues were collected with written informed consent from all donors and in accordance with the US Food and Drug Administration CFR Part 1271 Good Tissue Practices regulations. Tissue was processed as described elsewhere[46–48], and isolated hepatoblasts were seeded at density of 5.2×10^5 cm^{-2} on 12- or 24-well plates and in regular Kubota's Medium[49] supplemented with 5% FBS. Following an overnight incubation, the medium was changed to a variation of Kubota's Medium (HFH medium) comprised of DMEM supplemented with 25 mM HEPES, 1 nM selenium, 0.1% BSA, 4.5 mM niacinamide, 0.1 nM zinc sulfate heptahydrate, 10 nM hydrocortisone, 5 μg ml^{-1} transferrin/Fe, 5 μg ml^{-1} insulin, 2 mM L-glutamine, antibiotics and 2% FBS. The use of commercially procured fetal liver cells was reviewed by the University of North Carolina at Chapel Hill Office of Human Research Ethics and was determined not to require approval by the University of North Carolina at Chapel Hill Institutional Review Board.

Plasmids. pHJ3-5 (ref. 50), pHJ3-5/GLuc2A (referred to here as pHJ3-5/GLuc), pHJ3-5/GND, pH77c (ref. 51), pH77S.3, pH77S.3/GLuc2A (referred to here as pH77S.3/GLuc) and pH77S/GLuc2A-AAG (refs. 12,27,52) have been described. pHCV-N.2 is a modified version of HCV3-9b (ref. 32) that contains cell culture–adaptive mutations in NS3 and NS5A (A1099T, E1203G and S2204I in the polyprotein). Mutations in the sphingomyelin binding domain, 5′ UTR, 3′ UTR and nonstructural protein regions were generated by site-directed mutagenesis. The *Gaussia princeps* luciferase (GLuc)-coding sequence followed by the foot-and-mouth disease virus 2A protease–coding sequence was inserted between p7 and NS2 in pH77c, pHCV-N.2, pJFH1 (wild-type) and pJFH1-QL (containing the cell culture–adaptive mutation Q221L in the NS3 helicase) using a strategy applied previously to pH77S (ref. 27). JFH1-QL was used for experiments unless otherwise indicated. Other cell culture–adapted genotype 1a (TNcc), 2a (JFH-2/AS/mtT3), 3a (S52/SG-Feo(SH)) and 4a (ED43/SG-Feo(K)) HCV strains and RNA replicons have been described[34,53,54].

Luciferase assays. For the *Gaussia* luciferase (GLuc) assay, cells transfected with HCV RNA encoding GLuc were treated with drugs at 6 h after transfection, and the culture medium was harvested, refed with fresh medium containing drugs and assayed for GLuc at 24-h intervals. Secreted GLuc activity was measured as described[52]. For the firefly luciferase (FLuc) assay, cell monolayers were washed with PBS and lysed in Passive Lysis Buffer (Promega), and the lysates were analyzed with the Luciferase Assay System (Promega) according to the manufacturer's instructions. For each individual experiment, we used duplicate or triplicate cell cultures. Results shown represent the mean ± s.e.m. from multiple independent experiments.

RNA transcription. RNA transcripts were synthesized *in vitro* as described previously[27].

Hepatitis C virus RNA transfection. At 24 h before transfection, 7.5×10^4 Huh-7.5 cells were seeded onto a 24-well plate. One day later, medium was replaced with fresh medium, and the cells were transfected with 0.25 μg (per well) HCV RNA–encoding GLuc using the TransIT mRNA transfection kit (Mirus) according to the manufacturer's protocol. After 6 h incubation at 37 °C, supernatant fluids were removed for GLuc assay and replaced with fresh medium-containing compound. Alternatively, 10 μg of HCV RNA was mixed with 5×10^6 Huh-7.5 cells and electroporated into cells using a Gene Pulser Xcell Total System (Bio-Rad) as described previously[52]. Transfection of wild-type HCV RNA was performed by electroporating 5 μg HCV RNA in 2.5×10^6 Huh-7.5 cells and seeded into collagen-coated plates (BD Biosciences). Cells were grown in DMEM supplemented with 25 mM HEPES, 7 ng ml^{-1} glucagon, 100 nM hydrocortisone, 5 μg ml^{-1} insulin, 2 mM GlutaMAX, antibiotics and 2% FBS. Culture supernatants were replaced with the medium supplemented with drugs at 6 h and every 48 h thereafter and assayed for GLuc activity.

Hepatitis C virus production. For virus production, subconfluent Huh-7.5 cells in a 100-mm diameter dish were transfected with 5 μg HCV RNA using the TransIT mRNA transfection kit as above and split at 1:2 ratio at 6 h after transfection. Cells were then fed with medium supplemented with 50 mM HEPES (Cellgro) and the supernatants harvested and replaced with fresh medium every 24 h. Cells were passaged at a 1:2 ratio again 3 d after transfection. Medium containing HCV was supplemented with an additional 50 mM HEPES and stored at 4 °C until assayed for infectivity. *Gaussia* luciferase H77S.3/GLuc reporter virus was produced by electroporating 5 μg H77S.3/GLuc RNA into 2.5×10^6 Huh-7.5 cells. Cells were fed with medium containing 25 mM HEPES and 10 μM vitamin E at 3 h and grown for 3 d until subconfluent. Cells were then split 1:3 into medium containing 25 mM HEPES. Supernatant fluids, harvested on the following day, were stored at 4 °C until use. HJ3-5/GLuc virus was produced in medium lacking vitamin E and stored in −80 °C until use. Infectious titers were determined by $TCID_{50}$ using GLuc activity produced at 72 h after inoculation.

Hepatitis C virus infectivity assays. Huh-7.5 cells were seeded at 5×10^4 cells per well into 48-well plates 24 h before inoculation with 100 μl of culture medium. Cells were fed with medium containing 1 μM vitamin E 24 h later to facilitate visualization of core protein expression, fixed with methanol-acetone (1:1) at −20 °C for 10 min 72 h after inoculation (48 h for JFH1-QL and HJ3-5) and stained for intracellular core antigen with a mouse monoclonal antibody C7–50 (Thermo Scientific, 1:300 dilution). Clusters of infected cells identified by staining for core antigen were considered to constitute a single infectious focus, and the data were expressed as focus-forming units (FFU) ml^{-1}.

Hepatitis C virus infection in fetal hepatoblasts. Cells were inoculated with HCV encoding GLuc (MOI = 0.001) for 6 h. After washing five times with HFH medium, cells were incubated for an additional 18 h to determine baseline GLuc secretion. Culture supernatant fluids were replaced at 24 h intervals with HFH medium containing drugs and assayed for GLuc.

Flow cytometry. Huh-7.5 cells electroporated with H77S.3 or HJ3-5 RNA were treated with 1 μM SKI or DMSO beginning at 24 h and analyzed for NS5A expression by flow cytometry at 96 h. Virus spread assays were adapted from a previously described method[55]. Briefly, Huh-7.5 cells were electroporated with H77S.3, HJ3-5 or HJ3-5/GND RNAs and cultured for 24 h. The electroporated (producer) cells were then cocultured at a 1:4 ratio with naive Huh-7.5 (recipient) cells prelabeled with 5 μM carboxyfluorescein diacetate succinimidyl ester (CellTrace CFSE Cell Proliferation Kit, Invitrogen) in the presence of different compounds (see figure legends) for 48 h. Cells were stained for NS5A protein and analyzed by flow cytometry as described previously[56].

Equilibrium ultracentrifugation. Filtered supernatant fluids collected from transfected cell cultures were concentrated 50-fold using Centricon Plus-70 Centrifugal Filter Units (100-kDa exclusion) (Millipore) and then layered on top of a preformed continuous 10–40% iodixanol (OptiPrep, Sigma-Aldrich)

doi:10.1038/nm.3610

gradient in Hank's balanced salt solution (HBSS, Invitrogen). Gradients were centrifuged in a SureSpin 630 Swinging Bucket Rotor (Thermo Scientific) at 30,000 r.p.m. for 24 h at 4 °C, and fractions were collected from the top of the tube. The density of each fraction was calculated from the refractive index measured with a refractometer (ATAGO). RNA was isolated from each fraction using QIAamp Viral RNA kit (Qiagen) and the viral amount quantified by qRT-PCR as described below. Infectious virus titers in each fraction were determined as described above.

qRT-PCR. One-step qRT-PCR analysis of HCV RNA in Huh-7.5 cells was carried out as described[52]. HCV RNA in primary human fetal hepatoblast cultures was detected by means of a two-step qRT-PCR procedure using SuperScript III First-Strand Synthesis SuperMix for qRT-PCR (Invitrogen), followed by TaqMan qPCR analysis with primer pairs and a probe targeting a conserved 221-base sequence within the 5′ UTR of the genome and iQ Supermix (Bio-Rad)[52].

RNA interference. Validated siRNA targeting human *SPHK1* (SI02660455)[57] was purchased from Qiagen. siRNA targeting human *SPHK2* (5′-CGUCAC GGUUAAAGAGAAA-3′)[39] and control siRNA (#2) were from Dharmacon. siRNA (20 nM) was transfected into cells using siLentfect Lipid Reagent (Bio-Rad) according to the manufacturer's protocol.

Immunoblots. Immunoblotting was carried out using standard methods with the following antibodies: mouse monoclonal antibodies to β-actin (AC-74, Sigma, 1:10,000), HCV NS3 (ab65407, Abcam, 1:500) and rabbit polyclonal antibodies to SPHK1 (A302-177A, Bethyl Laboratories, 1:2,000) or SPHK2 (ab37977, Abcam, 1:500). Protein bands were visualized and quantified with an Odyssey Infrared Imaging System (Li-Cor Biosciences).

Sphingosine kinase assay. Sphingosine kinase activity was determined as described previously[28]. Recombinant human SPHK1 and SPHK2 proteins were obtained from BPS Bioscience. SPHK1 activity was determined in the presence of 0.25% Triton X-100, which inhibits SPHK2 (ref. 28). The labeled S1P was separated by TLC on Silica Gel G-60 (Whatman) with 1-butanol/ethanol/acetic acid/water (80:20:10:20, v/v) and visualized and quantified by phosphorimager (Bio-Rad).

Quantification of cholesterol and triglyceride levels. Cells were scraped and lysed in PBS containing 1% Triton X-100 and complete protease inhibitor cocktail (Roche). Cell lysates were clarified by centrifugation at 15,000 r.p.m. at 4 °C for 10 min. Cholesterol contents were determined using the Amplex Red Cholesterol Assay Kit (Invitrogen) according to the manufacturer's protocol. Triglyceride levels in cells grown on 96-well plates were determined using Triglyceride Assay Kit (Zen-Bio) as per manufacturer's instruction. The values were normalized to the total protein content.

Lipid peroxidation assays. Malondialdehyde (MDA), a product of lipid peroxidation, was quantified by the thiobarbituric acid reactive substances (TBARS) Assay Kit (Cayman Chemical). Cells transfected with HCV RNAs were grown in the presence of different drugs and analyzed for intracellular malondialdehyde (MDA) abundance at 48–72 h as indicated in legends. Cells scraped into PBS containing complete protease inhibitor cocktail (Roche) were homogenized by sonication on ice using Sonic Dismembrator (FB-120, Fisher Scientific). The amount of MDA in 100 µl of cell homogenates was analyzed by a fluorescent method as described by the manufacturer. Lipid peroxidation levels were expressed as the amount of MDA normalized to the amount of total protein. Alternatively, the lipid peroxidation product, 8-isoprostane, was quantified using the 8-Isoprostane EIA kit (Cayman Chemical) according to the manufacturer's recommended procedures.

Innate immune response reporter assays. IFN-β–, IRF-3– and NF-κB–dependent promoter activities were assayed using firefly luciferase reporters pIFN-β-Luc, p4xIRF3-Luc or pPRDII-Luc as described previously[58]. Cells were cotransfected with the reporter plasmid pRL-CMV, and the firefly luciferase results were normalized to *Renilla* luciferase activity in order to control for potential differences in transfection efficiency. The luminescence was measured on a Synergy 2 (Bio-Tek) Multi-Mode Microplate Reader.

Mass spectrometry of sphingolipids and metabolites. Cells were washed extensively with PBS and scraped into tubes. An aliquot of cells was taken for protein and total lipid phosphate measurements. After addition of a sphingolipid internal standard cocktail (Avanti Polar Lipids), the lipids were extracted, and individual sphingolipid species were quantified by liquid chromatography, electrospray ionization-tandem mass spectrometry as described previously[59,60].

Electron microscopy. Huh-7.5 cells (5×10^6 cells) electroporated with 5 µg HCV RNA were seeded into a 6-well plate, and medium containing compounds was added 24 h later. At 48 h after transfection, cells were fixed with 3% glutaraldehyde in 0.15 M sodium phosphate buffer, pH 7.4, for 1 h at room temperature and stored at 4 °C until processed. Following three rinses with 0.15 M sodium phosphate buffer, pH 7.4, monolayers were postfixed with 1% osmium tetroxide for 1 h, washed in deionized water and stained *en bloc* with 2% aqueous uranyl acetate for 20 min. The cells were dehydrated using increasing concentrations of ethanol (30%, 50%, 75%, 100%, 100%, 10 min each) and embedded in Polybed 812 epoxy resin (Polysciences, Inc.). Cell layers were sectioned *en face* to the substrate at 70 nm using a diamond knife and a Leica Ultracut UCT microtome (Leica Microsystems). Ultrathin sections were mounted on 200 mesh copper grids and stained with 4% aqueous uranyl acetate and Reynolds' lead citrate[61]. The grids were observed at 80 kV using a LEO EM910 transmission electron microscope (Carl Zeiss SMT, LLC). Digital images were taken using a Gatan Orius SC 1000 CCD Camera with DigitalMicrograph 3.11.0 software (Gatan, Inc.).

Peroxidation resistance of hepatitis A virus, flavivirus, alphavirus and lymphocytic choriomeningitis virus replicases. Virus stocks were provided as follows: HAV by Z. Feng and S.M.L.; YFV and WNV by D.P.D.; DENV by D.G.W.; SINV, RRV and CHIKV by M.T.H.; and LCMV by J.K.W. The abundance of HAV, RRV, SINV and LCMV RNA was determined using iScript One-Step RT-PCR kit with SYBR green (Bio-Rad) and primer pairs as follows: HAV forward 5′-GGTAGGCTACGGGTGAAAC-3′ and reverse 5′-AACAACTCACCAATATCCGC-3′, RRV forward 5′-AGAGT GCGGAAGACCCAGAG-3′ and reverse 5′-CCGTGATCTTACCGGACA CA-3′, SINV forward 5′-GAGGTAGTAGCACAGCAGG-3′, and reverse 5′-CG GAAAACATTCTACGAGC-3′ and LCMV forward 5′-CATTCACCTGGACTTT GTCAGACTC-3′ and reverse 5′-GCAACTGCTGTGTTCCCGAAAC-3′. WNV and YFV RNA levels were quantified using a previously described method[62] with primers as follows: WNV forward 5′-TCAGCGATCTCTCCACCAAAG-3′ and reverse 5′-GGGTCAGCACGTTTGTCATTG-3′ and YFV forward 5′-CT GTCCCAATCTCAGTCC-3′ and reverse 5′-AATGCTCCCTTTCCCAAA TA-3′. DENV RNA was quantified on a 7900 HT Real-Time PCR System (ABI) using primers and probe as described[63].

The infrared fluorescent immunofocus assay for infectious hepatitis A virus (HAV) was done using FRhK-4 cells as previously described[64]. Titration of infectious alphaviruses was performed in duplicate by visualization of plaques on Vero cells seeded in 12-well plates. Plates were incubated with inoculum at 37 °C with 5% CO_2 for 1 h with periodic agitation. Inocula were then removed and plates overlaid with 1.25% carboxymethylcellulose in MEM supplemented with 3% FBS, 1× penicillin-streptomycin, 2 mM L-glutamine and HEPES. All of these reagents were identical to those used for parallel studies of HCV. At 48 h after infection, plates were fixed with 4% paraformaldehyde and visualized with a 0.25% crystal violet solution. Infectious titers of WNV and YFV were determined by plaque assay on confluent BHK cell monolayers in 6-well plates. Cells were incubated with virus inocula for 2 h at 37 °C, washed before addition of a 1% methylcellulose medium overlay and further incubated for 3 d. Plaques were visualized with Giemsa staining. DENV titers were determined by plaque assay on Vero 76 cell monolayers in 96-well plates. Cells were incubated with virus inocula for 2 h at 37 °C, washed before addition of a 0.8% methylcellulose medium overlay and further incubated for 3 d. Following fixation with ice-cold acetone methanol solution (50:50 v/v), cells were immunostained using the DENV E-specific monoclonal antibody 4G2 (UNC Antibody Core Facility, 1:500) followed by HRP-conjugated anti-mouse IgG secondary antibody (KPL, 464-1806, 1:1,000). Infectious foci were visualized using Vector VIP reagent (Vector Labs). LCMV titers were determined by plaque assay on confluent Vero cell monolayers in 6-well plates[65]. Cells were incubated with virus inocula for 80 min at 37 °C before addition of a 1:1 mixture of 1% agarose and EMEM medium containing 10% FCS, 2 mM L-glutamine, 2% penicillin and

2% streptomycin. Cells were further incubated for 5 d at 37 °C. Plaques were visualized with crystal violet.

Modeling of hepatitis C virus nonstructural protein-membrane interactions. Membrane topologies of HCV nonstructural proteins were modeled as suggested by Bartenschlager *et al.*[66] using the Protein Data Bank (PDB) structure 4A92 for the NS3-4A protease-helicase (**Fig. 6c**) and PDB 1GX6 for the NS5B RNA-dependent RNA polymerase (**Fig. 6c**). Secondary structure predictions were generated on the Jpred3 server (http://www.compbio.dundee.ac.uk/www-jpred/). Visual Molecular Dynamics (VMD) with the plugin "Membrane" was applied for visualization of protein-membrane interactions[67].

Statistical analyses. Unless noted otherwise, all between-group comparisons were carried out by two-way ANOVA using Prism 6.0 software (GraphPad Software, Inc.). For determination of EC_{50} concentrations of DAAs, data were fit to a four-parameter dose-response curve with variable slope using Prism 5.0c for Mac OS X software (GraphPad Software, Inc.). Results are reported as the estimated $EC_{50} \pm 95\%$ confidence interval (**Fig. 5g**).

45. Leivers, A.L. *et al.* Discovery of selective small molecule type iii phosphatidylinositol 4-kinase α (PI4KIIIα) inhibitors as anti hepatitis C (HCV) agents. *J. Med. Chem.* **57**, 2091–2106 (2014).
46. Oikawa, T. *et al.* Sal-like protein 4 (SALL4), a stem cell biomarker in liver cancers. *Hepatology* **57**, 1469–1483 (2013).
47. Schmelzer, E. *et al.* Human hepatic stem cells from fetal and postnatal donors. *J. Exp. Med.* **204**, 1973–1987 (2007).
48. Wang, Y. *et al.* Paracrine signals from mesenchymal cell populations govern the expansion and differentiation of human hepatic stem cells to adult liver fates. *Hepatology* **52**, 1443–1454 (2010).
49. Kubota, H. & Reid, L.M. Clonogenic hepatoblasts, common precursors for hepatocytic and biliary lineages, are lacking classical major histocompatibility complex class I antigen. *Proc. Natl. Acad. Sci. USA* **97**, 12132–12137 (2000).
50. Ma, Y., Yates, J., Liang, Y., Lemon, S.M. & Yi, M. NS3 helicase domains involved in infectious intracellular hepatitis C virus particle assembly. *J. Virol.* **82**, 7624–7639 (2008).
51. Yanagi, M., Purcell, R.H., Emerson, S.U. & Bukh, J. Transcripts from a single full-length cDNA clone of hepatitis C virus are infectious when directly transfected into the liver of a chimpanzee. *Proc. Natl. Acad. Sci. USA* **94**, 8738–8743 (1997).
52. Shimakami, T. *et al.* Stabilization of hepatitis C virus RNA by an Ago2–miR-122 complex. *Proc. Natl. Acad. Sci. USA* **109**, 941–946 (2012).
53. Date, T. *et al.* Novel cell culture-adapted genotype 2a hepatitis C virus infectious clone. *J. Virol.* **86**, 10805–10820 (2012).
54. Saeed, M. *et al.* Efficient replication of genotype 3a and 4a hepatitis C virus replicons in human hepatoma cells. *Antimicrob. Agents Chemother.* **56**, 5365–5373 (2012).
55. Timpe, J.M. *et al.* Hepatitis C virus cell-cell transmission in hepatoma cells in the presence of neutralizing antibodies. *Hepatology* **47**, 17–24 (2008).
56. Kannan, R.P., Hensley, L.L., Evers, L.E., Lemon, S.M. & McGivern, D.R. Hepatitis C virus infection causes cell cycle arrest at the level of initiation of mitosis. *J. Virol.* **85**, 7989–8001 (2011).
57. Puneet, P. *et al.* SphK1 regulates proinflammatory responses associated with endotoxin and polymicrobial sepsis. *Science* **328**, 1290–1294 (2010).
58. Dansako, H. *et al.* Class A scavenger receptor 1 (MSR1) restricts hepatitis C virus replication by mediating toll-like receptor 3 recognition of viral RNAs produced in neighboring cells. *PLoS Pathog.* **9**, e1003345 (2013).
59. Shaner, R.L. *et al.* Quantitative analysis of sphingolipids for lipidomics using triple quadrupole and quadrupole linear ion trap mass spectrometers. *J. Lipid Res.* **50**, 1692–1707 (2009).
60. Sullards, M.C., Liu, Y., Chen, Y. & Merrill, A.H. Jr. Analysis of mammalian sphingolipids by liquid chromatography tandem mass spectrometry (LC-MS/MS) and tissue imaging mass spectrometry (TIMS). *Biochim. Biophys. Acta* **1811**, 838–853 (2011).
61. Reynolds, E.S. The use of lead citrate at high pH as an electron-opaque stain in electron microscopy. *J. Cell Biol.* **17**, 208–212 (1963).
62. Papin, J.F., Vahrson, W. & Dittmer, D.P. SYBR green-based real-time quantitative PCR assay for detection of West Nile Virus circumvents false-negative results due to strain variability. *J. Clin. Microbiol.* **42**, 1511–1518 (2004).
63. Gurukumar, K.R. *et al.* Development of real time PCR for detection and quantitation of Dengue Viruses. *Virol. J.* **6**, 10 (2009).
64. Qu, L. *et al.* Disruption of TLR3 signaling due to cleavage of TRIF by the hepatitis A virus protease-polymerase processing intermediate, 3CD. *PLoS Pathog.* **7**, e1002169 (2011).
65. Ahmed, R., Salmi, A., Butler, L.D., Chiller, J.M. & Oldstone, M.B. Selection of genetic variants of lymphocytic choriomeningitis virus in spleens of persistently infected mice. Role in suppression of cytotoxic T lymphocyte response and viral persistence. *J. Exp. Med.* **160**, 521–540 (1984).
66. Bartenschlager, R., Lohmann, V. & Penin, F. The molecular and structural basis of advanced antiviral therapy for hepatitis C virus infection. *Nat. Rev. Microbiol.* **11**, 482–496 (2013).
67. Humphrey, W., Dalke, A. & Schulten, K. VMD: visual molecular dynamics. *J. Mol. Graph.* **14**, 33–38, 27–28 (1996).

JVI
Journals.ASM.org

hnRNP L and NF90 Interact with Hepatitis C Virus 5′-Terminal Untranslated RNA and Promote Efficient Replication

You Li, Takahiro Masaki, Tetsuro Shimakami,* Stanley M. Lemon

Departments of Medicine and Microbiology Immunology, and Lineberger Comprehensive Cancer Center, The University of North Carolina at Chapel Hill, Chapel Hill, North Carolina, USA

ABSTRACT

The 5′-terminal sequence of the hepatitis C virus (HCV) positive-strand RNA genome is essential for viral replication. Critical host factors, including a miR-122/Ago2 complex and poly(rC)-binding protein 2 (PCBP2), associate with this RNA segment. We used a biotinylated RNA pulldown approach to isolate host factors binding to the HCV 5′ terminal 47 nucleotides and, in addition to Ago2 and PCBP2, identified several novel proteins, including IGF2BP1, hnRNP L, DHX9, ADAR1, and NF90 (ILF3). PCBP2, IGF2BP1, and hnRNP L bound single-stranded RNA, while DHX9, ADAR1, and NF90 bound a cognate double-stranded RNA bait. PCBP2, IGF2BP1, and hnRNP L binding were blocked by preannealing the single-stranded RNA bait with miR-122, indicating that they bind the RNA in competition with miR-122. However, IGF2BP1 binding was also inhibited by high concentrations of heparin, suggesting that it bound the bait nonspecifically. Among these proteins, small interfering RNA-mediated depletion of hnRNP L and NF90 significantly impaired viral replication and reduced infectious virus yields without substantially affecting HCV internal ribosome entry site-mediated translation. hnRNP L and NF90 were found to associate with HCV RNA in infected cells and to coimmunoprecipitate with NS5A in an RNA-dependent manner. Both also associate with detergent-resistant membranes where viral replication complexes reside. We conclude that hnRNP and NF90 are important host factors for HCV replication, at least in cultured cells, and may be present in the replication complex.

IMPORTANCE

Although HCV replication has been intensively studied in many laboratories, many aspects of the viral life cycle remain obscure. Here, we use a novel RNA pulldown strategy coupled with mass spectrometry to identify host cell proteins that interact functionally with regulatory RNA elements located at the extreme 5′ end of the positive-strand RNA genome. We identify two, primarily nuclear RNA-binding proteins, hnRNP L and NF90, with previously unrecognized proviral roles in HCV replication. The data presented add to current understanding of the replication cycle of this pathogenic human virus.

Hepatitis C virus (HCV) is a leading cause of liver disease, including chronic hepatitis, cirrhosis, and hepatocellular carcinoma. It is classified within the *Flaviviridae* family of viruses and has a single-stranded, messenger-sense RNA genome ~9.7 kb in length. The replication of HCV viral RNA is uniquely dependent on a host-factor microRNA (miRNA), miR-122, which is highly abundant in liver (1, 2). There are two conserved miR-122 binding sites (S1 and S2) located near the 5′ end of the positive-sense HCV RNA genome. Direct interactions between miR-122, and these sites are essential for the HCV life cycle (3, 4). This is reflected clinically in dose-dependent reductions of circulating HCV RNA after intravenous administration of an antisense miR-122 "antagomir" to HCV-infected chimpanzees and humans (5, 6).

Previous studies demonstrate that binding of miR-122 to the 5′-untranslated region (5′UTR) of the HCV genome stimulates viral protein expression (7, 8) and also physically stabilizes the RNA in infected cells (9, 10). Similar to conventional miRNA action, miR-122 recruits Argonaute 2 protein (Ago2) to the viral RNA (9, 11). The stability conferred by the miR-122/Ago2 complex can be substituted functionally by addition of a 5′ cap, suggesting that it protects against 5′-exonuclease-mediated decay (9). Indeed, studies of RNA decay pathways have revealed that HCV RNA is primarily degraded from the 5′ end by the exonuclease Xrn1 in infected cells and that the binding of miR-122 to the HCV 5′UTR effectively blocks Xrn1-mediated degradation (10). However, depletion of Xrn1 in Huh-7.5 cells failed to rescue the replication of HCV RNA containing single-base substitutions in both S1 and S2 that ablate miR-122 binding, suggesting that miR-122 has an additional, essential role in HCV replication beyond protecting the RNA genome from Xrn1-mediated degradation (10).

The 5′UTR of HCV folds into conserved stem-loops (SL1 to SL4), with SL2 to SL4 participating in HCV internal ribosome entry site (IRES)-directed translation (12, 13). The 5′UTR serves as a platform to recruit proteins that are essential for viral protein synthesis and RNA replication. Cellular RNA-binding proteins, including eukaryotic initiation factor 3 (eIF3), the 40S ribosomal subunit, polypyrimidine-tract-binding protein (PTB), poly(rC)-binding protein 2 (PCBP2), and La autoantigen, have been shown to bind to the 5′UTR of HCV RNA and to play important roles in viral translation and/or replication (14–18). The miR-122 binding sites (S1 and S2) are located upstream of SL2, encompassing the

Received 23 January 2014 Accepted 6 April 2014
Published ahead of print 9 April 2014
Editor: B. Williams
Address correspondence to Stanley M. Lemon, smlemon@med.unc.edu.
* Present address: Tetsuro Shimakami, Department of Gastroenterology, Kanazawa University Graduate School of Medicine, Takara-Machi, Japan.

doi:10.1128/JVI.00225-14